Adaptive mesh refinement in flood simulations – a case study in an alpine river

Michaela Sichert[1]

[1]Z_GIS, University of Salzburg, Austria·Michaela.Sichert@stud.sbg.ac.at

Abstract

Within the last decades, numerical simulations have become an important method for decision-making on flood prevention as well as for understanding the alteration of riverine landscapes. However, modelling flood events require high computational costs. The advantages of adaptive mesh refinement in comparison to non-adaptive uniform grids have been well researched in recent years. The aim of this study, however, was to compare the computational efficiency of an adaptive mesh refinement hydraulic model with a non-uniform non-adaptive counterpart in an alpine environment. Two hydraulic models were thus generated with the Gerris Flow Solver, using 2D shallow water equations and quadtree grids. By simulating a single flood event, the outcomes of the two hydraulic models were compared with regard to the computational costs as well as the accuracy. The adaptive mesh refinement model requires 35 % more cells and 54 % more CPU time. Nevertheless, the analysis of two different hydraulic parameters at homologous sites and time steps revealed that the accuracy in terms of information density is higher in the adaptive mesh refinement model. Although the proposed hydraulic models in this study refer to a channel section of the Taugl River, they are transferable to other study sites. The results thus contribute to the research on the computational efficiency of flood simulations in alpine environments.

1 Introduction

As a consequence of climate change, the number of natural hazards like flood events has risen considerably in recent years (Anees et al., 2016; Gong, Shimizu, & Iwasaki, 2020). Especially in mountainous regions, floods are very devastating as they can reach high peak flows. Despite this fact, flooding in alpine rivers is poorly researched yet (Hou et al., 2019). In general, flood events are not only subject in the field of fluvial geomorphology in order to understand the alteration of riverine landscapes (Baynes et al., 2015; Coulthard & Van De Wiel, 2013), but also constitute a restrictive factor with regard to the economy and society in catchment areas (Hou et al., 2019). Numerical simulations are thus an important method for flood risk assessment and management (An, Yu, Lee, & Kim, 2015) as well as for research in the field of geomorphology (Coulthard & Van De Wiel, 2013). However, accurate and efficient hydraulic models are crucial in order to simulate floods accurately (Qiuhua Liang, Du, Hall, & Borthwick, 2008).

The advancement of technology and numerical algorithms in recent decades has led to the establishment of various 2D and 3D fluid dynamic models (Coulthard & Van De Wiel, 2013; Darby & Van de Wiel, 2003; Huang, Cao, Pender, Liu, & Carling, 2015). In comparison to 1D models, they are able to simulate the flood dynamics even in complex scenarios more precise (Kirstetter, Bourgin, Brigode, & Delestre, 2020). However, accurate and reliable

simulation outcomes are dependent on an appropriately high mesh resolution whereby modelling flood events require high computational costs (Huang et al., 2015). By implementing adaptive mesh refinement (AMR), the computational efficiency of numerical flood simulations can be enhanced (An et al., 2015; J. P. Wang & Liang, 2011). This approach was proposed by Berger and Oliger (1984) and is particularly convenient when the solution of the models is discontinuous or unevenly distributed in the simulation domain. AMR adapts the mesh in every time step in which the simulated fluid develops, since high-resolution is only necessary within a minor part of the simulation domain. For the remaining area a lower resolution is appropriate (Huang et al., 2015). Because the flooded sites that are to be resolved in a high resolution evolve dynamically, adapting the grid is a time-dependent approach (Berger & Oliger, 1984). Hence only the relevant areas within the simulation domain are refined, AMR reduce the computational costs without compromising the accuracy of the simulation results (Gong et al., 2020; Huang et al., 2015; J. P. Wang & Liang, 2011). AMR is becoming more common in hydraulic modelling (e.g., Hu et al., 2019; Q. Liang, Borthwick, & Stelling, 2004; J. P. Wang & Liang, 2011), since a mesh that automatically refines itself is recommended for simulating complicated flow geometries that evolve dynamically (Borthwick, Cruz Leon, & Józsa, 2001).

One efficient way to apply AMR is by implementing an adaptive quadtree grid (An et al., 2015; J. P. Wang & Liang, 2011), which is recently applied in various studies (e.g., Kesserwani & Liang, 2012; Q. Liang et al., 2004; Qiuhua Liang et al., 2008; Qiuhua Liang, Zang, Borthwick, & Taylor, 2007; S. Popinet, 2012). By using this technique, the simulation domain is discretised into hierarchically organized square finite volumes (Stéphane Popinet, 2003). A quadtree grid is thus constructed from a vast number of automatically generated non-uniform Cartesian cells (Qiuhua Liang et al., 2007). The corresponding indexing system refers to a tree structure in order to assign the information to the finite volumes (Borthwick et al., 2001). Adaptive quadtree grids represent a suitable solutions for issues regarding the local cell resolution (Qiuhua Liang et al., 2008). It is a straightforward technique to discretize the simulation domain into several sub-quadrants (Borthwick et al., 2001). Whether a cell is further subdivided is controlled by the user who applies customized conditions that need to be fulfilled for further cell discretization (Qiuhua Liang et al., 2008; Qiuhua Liang et al., 2007). As a result, the mesh is locally adaptable (Borthwick et al., 2001) according to the user requirements (Qiuhua Liang et al., 2008). Thereby, the efficiency as well as the accuracy of the hydraulic model is enhanced (An & Yu, 2012; Borthwick et al., 2001). According to several studies (e.g., Qiuhua Liang et al., 2007; J. Wang, Borthwick, & Taylor, 2004; J. P. Wang & Liang, 2011), the computational efficiency of hydraulic models can thus be increased by implementing adaptive quadtree grids instead of non-adaptive uniform ones. The main reason for this is that a uniform high-resolution grid drastically increases the computational time (Hu, Fang, Salinas, & Pain, 2018).

In the scope of this study, the effects of AMR on the computational efficiency are investigated in an alpine environment with regard to computational time and resolution of different hydraulic parameters. To accomplish this, two fluid dynamic models based on the 2D nonlinear shallow water equations are developed with the Gerris Flow Solver for a channel section of the torrent Taugl River in the province of Salzburg. The aim of this study is to analyse and quantify the impacts on the computational efficiency of single flood simulations by applying AMR, motivated by the fact that only few research has done this so far for flood events in alpine environments. This required the comparison of the model results obtained from AMR with results derived from a static (i.e. non-adaptive) mesh refinement (SMR). In

contrast to the majority of recent studies (e.g., Gong et al., 2020; J. P. Wang & Liang, 2011), the differences between a non-uniform SMR and AMR are analysed here. Both applied methods of mesh refinement rely on a quadtree grids. By simulating single floods based on SMR as well as on AMR, the research questions whether and which effects on the computational costs and on the accuracy (i.e. information density) of various hydraulic parameters occur is answered.

2 Material and Methods

2.1 Study site

The study site is a channel section of the Taugl River (Figure **1**). As part of the Taugl River catchment, the area of interest is positioned in the south-western edge of the Osterhorn Group in the Northern Calcareous Alps in the Salzburger Land (Guttmann, 1997).

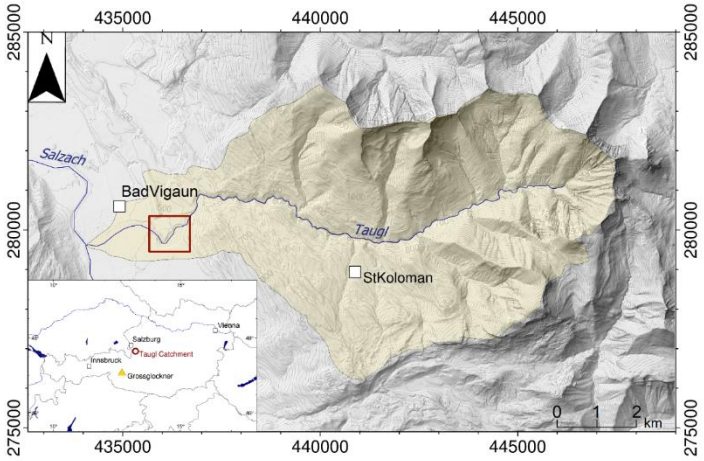

Figure 1: Location of the study site (red rectangle), positioned within Taugl River catchment (golden area). The location of the Taugl catchment (red circle) within Austria (grey outlines) is shown within the inset.

2.2 Gerris Flow Solver

The Gerris Flow Solver (GFS) is an open source software system developed by Stèphane Popinet (Keen, Campbell, Dykes, & Martin, 2013). GFS was established for solving the incompressible Euler equation, but was enhanced to further models including shallow water equations (SWE) (1). The software features a second-order precise Gudunov type as shallow water flow solver (An et al., 2015). GFS uses a command line. The code is stored within a parameter file. Functions within the parameter file are defined with the C programming language (Stèphane Popinet, 2004).

2.2.1 Governing equations

The governing equations of this study are the 2D non-linear SWE based on a Cartesian coordinate system (x, y, z) (An et al., 2015). Those equations refer recently to the state-of-the-art of flood simulation techniques (J. P. Wang & Liang, 2011). The SWE are the 2D depth-averaged derivation from the 3D Navier-Stokes equations (Coulthard & Van De Wiel, 2013; Hergarten & Robl, 2015). They are based on a horizontal water layer allowing to neglect the vertical velocity but integrate the depth averaged horizontal velocities (υ_h). Thereby the hydrostatic pressure is integrated instead of the vertical one (Grenfell, 2015; Hergarten & Robl, 2015). This concept is based on the assumption that the horizontal plane (i.e. the floodplain) is significantly larger than the vertical plane (i.e. the water depth) (Qiuhua Liang et al., 2008). The SWE include a 2D gradient operator (∇) and are calculated as follows:

$$\frac{\partial}{\partial_t} v_h + (\upsilon_h * \nabla) v_h = gs - \frac{\tau}{\rho h_v} \frac{\upsilon_h}{|\upsilon_h|} \quad (1)$$

Friction is included in the second half of the equation. Here, τ is the basal shear stress, g is the gravitational acceleration, s is the negative gradient of the water layer, ρ refers to the bulk density and h_v is the vertical flow depth (Hergarten & Robl, 2015).

2.2.2 Adaptive quadtree grid refinement

The GFS features AMR based on adaptive quadtree grids (An & Yu, 2012). In 2D models, the simulation domain is spatially decomposed into square finite volumes (i.e. into cells). The sub-quadrants can be hierarchically organized in the form of a quadtrees (Stéphane Popinet, 2003). Generating the quadtree grid is based on the automatic discretization of the unit square cell, which is also referred as root cell. The mesh is thus composed of various non-uniform Cartesian cells (Qiuhua Liang et al., 2007). Starting from the root cell with a level of zero, further levels are added with increasing discretization. Overall, each parent cell can be divided into four children cells. Quadtree grids can thereby be described in terms of levels and the parent-children concept (An & Yu, 2012). When generating the quadtree grid, the boundary geometry of the entire simulation domain is rescaled initially in order to match the root cell (Qiuhua Liang et al., 2007). An adaptation indicator must be determined so that the mesh is dynamically adapted during the simulation (i.e. refinement and coarsening). There is no universal one, instead the indicator can be tailored to the study (Huang et al., 2015). For instance, J. P. Wang and Liang (2011) used a specific water surface gradient as an indicator. A detailed description of adaptive grid refinement is provided by An and Yu (2012).

2.3 Computational condition

In the scope of this study, flood simulations based on quadtree grids were performed in a torrent. The main objective was to explore the impact of AMR on computational costs and the accuracy of hydraulic parameters in terms of information density in an alpine environment. To achieve this, a hydraulic model based on AMR as well as one based on non-uniform SMR were developed. Besides the different methods for implementing the mesh refinements, all other simulation parameters were kept constant. In this way, it is ensured that only the effects of adaptivity cause different simulation results. Both hydraulic models were validated based on the total water volume in every time step (Stéphane Popinet, 2012). Since it is advantageous to automatically derive information about hydraulic parameters at specific

sites, virtual data logger in form of two profiles were implemented across the channel. **Fehler! Verweisquelle konnte nicht gefunden werden.** summarizes the computational conditions for both hydraulic models. The simulation domain width, the resolution of the topographic input, the discharge, the duration of the simulation and the friction model based on a constant hydraulic roughness parameter remain the same. However, due to the different methods of mesh refinement, the minimum level varies between SMR and AMR.

Table 1: Computational conditions of the hydraulic models.

Computational domain width		1431 m
Resolution of topographic input		1 m
Discharge (constant inflow)		100 m³/s
Friction model		Smart, Duncan and Walsh (2002)
Constant hydraulic roughness		0.01 m
Non-adaptive quadtree grid	min. refinement level	4
	max.refinement level	10
Adaptive quadtree grid	min. refinement level	2
	max. refinement level	10
Calculation end time		1000 s

For setting up an executable flood simulation file, a digital elevation model (DEM) was required that is used as physical representation of space (Darby & Van de Wiel, 2003). The DEM was provided by the state government of Salzburg. It was acquired in 2013 and has a spatial resolution of 1 m (**Fehler! Verweisquelle konnte nicht gefunden werden.**). Since a DEM is not readable for Gerris in a common shapefile format, a conversion into a 2D tree-indexed terrain database (quadtree) is required (Keen et al., 2013). Afterwards, the DEM can be used to determine the simulation domain (Stéphane Popinet, 2012). A constant discharge of 100 m³/s was specified and fed into the simulation domain at a certain position (436874, 280543). In order to increase the accuracy of the hydraulic models, the Smart, Duncan, and Walsh (2002) friction model was implemented. A constant hydraulic roughness parameter of 0.01 m was applied, since the resolution of the used DEM is not sufficient to approach the bed roughness as described by Smart et al. (2002).

For simulations based on SMR, a non-uniform quadtree grid was defined based on two conditions. The highest refinement level of ten should be generated in both, a circular area around the inflow point and in sites where the terrain reconstruction error is larger than 0.75 m. The first condition is related to the fact that the inflow area represents an important zone for flood simulations and should thus be resolved to the highest level. The second condition deals with the requirement of a high resolution in sites that are more complex in terms of topography. The terrain reconstruction error results from residuals of the recursive quadtree

grid refinement by a least-square bilinear approximation of the topography (Bertram & Tricoche, 2003).

Within the AMR hydraulic model, the mesh is refined in every time step up to a maximum level of ten if a cell is either inundated or located within the circular inflow area. A cell is considered as flooded if the water depth is larger than 0.001 m. Overall, by evaluating the conditions in each time step, the quadtree grid is dynamically adapted to the evolving flood. In order to prevent an initial slow calculation, a uniform quadtree grid with 16 x 16 cells was determined as an initial mesh, which is refined when starting the simulation (Stéphane Popinet, 2012).

3 Results

The SMR as well as the AMR hydraulic model were validated based on the total amount of water within the simulation domain in every time step until the calculation end time. A linear increase of the fluid volume results in both cases (Figure 2).

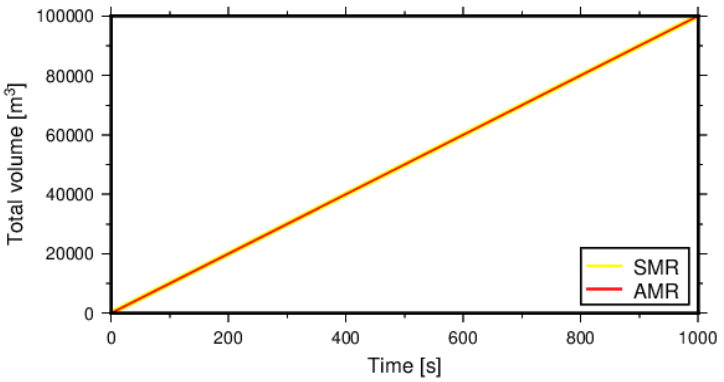

Figure 2: Total volume [m³] of water per time step [s] for the SMR (yellow line) and the AMR (red line) model.

3.1 Non-uniform quadtree grids

Figure 3 shows the resulting quadtree grids. Since the mesh of the AMR model is dynamically refined in every time step, the final result after the calculation end time (Table 1) is presented. It is apparent that the quadtree grid resulting from AMR only reaches the highest level of refinement in a certain region of the simulation domain. With increasing distance to this site, the mesh becomes coarser. When comparing the area with the highest refinement level resulting from the AMR model with the quadtree grid derived from the SMR counterpart, it is discernible that the same region is rather coarse resolved. Overall, SMR leads to various smaller sites with high refinement level distributed across the entire simulation domain.

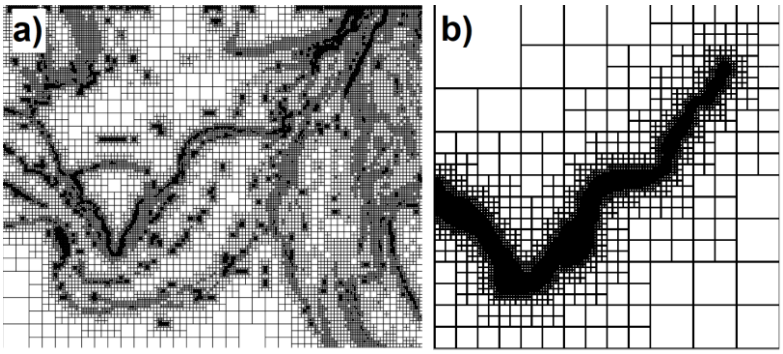

Figure 3: Non-uniform a) non-adaptive and b) adaptive quadtree grid resulting from SMR and AMR, respectively.

3.2 Effects on the computational costs

In order to analyse the effects on the computational cost due to the usage of adaptivity, the resulting CPU time should be compared between the models based on SMR and AMR (Figure 4). It is recognisable that the required CPU time for a simulation based on SMR increases linearly. In contrast, the needed time initially increases exponential and from about 800 s onwards linear in the AMR model. Overall, a flood simulation based on SMR requires approx. 3250 s and 5000 s when applying AMR. Thus, the simulation based on AMR needs about 1750 s more CPU time, even though it was less time-consuming until a time step of 650 s.

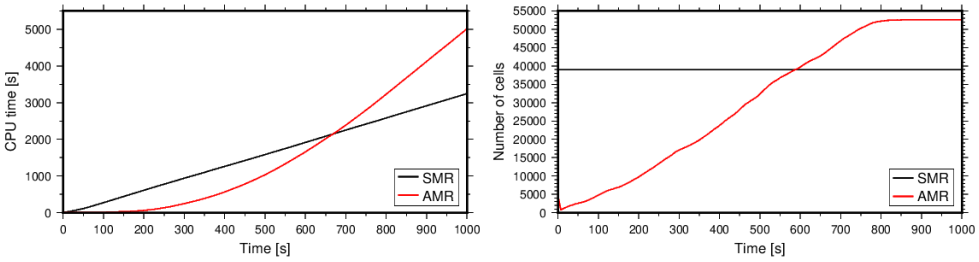

Figure 4: CPU time [s] (left) and number of cells per time step [s] for simulations based on SMR (black line) and AMR (red line) while all other parameters were kept constant.

Since only the method of mesh refinement is modified while all other parameters were kept constant (Table 1), the resulting cell number (Figure **4**) should also be taken into account in relation to the required CPU time. In the SMR model, the cell number remains constant with 38920 cells during the whole simulation. In contrast, the amount in the AMR model changes dynamically over time. It is apparent that the number varies less strongly from about 800 s onwards. The maximum number of cells after 1000 s is 52615. It is striking that the number of cells initially decreases when the initial mesh is refined for the first time. Overall, the AMR model consists of 13695 cell than the SMR counterpart.

3.3 Impacts on the accuracy

When comparing the predicted water depth between simulations based on SMR and AMR at different time steps, the impacts of adaptivity on the accuracy in terms of information density can be revealed (Figure 5). The simulated water depth obtained from simulations based on SMR shows that the entire channel width is flooded. Consequently, no river branches are discernible and the simulated result appears blurred. In the simulation results based on AMR, it is apparent that several secondary channels separate from the main stream. As a result, a braided river system is modelled consisting of some dry or only slightly flooded areas between the channels. Comparatively fewer sites are inundated consequently. This observation can be confirmed by calculating the flooded areas in different time steps for simulations based on SMR and AMR. Table **2** shows the inundated sites after 600 s and 1000 s. In both cases, the flooded area resulting from SMR is larger.

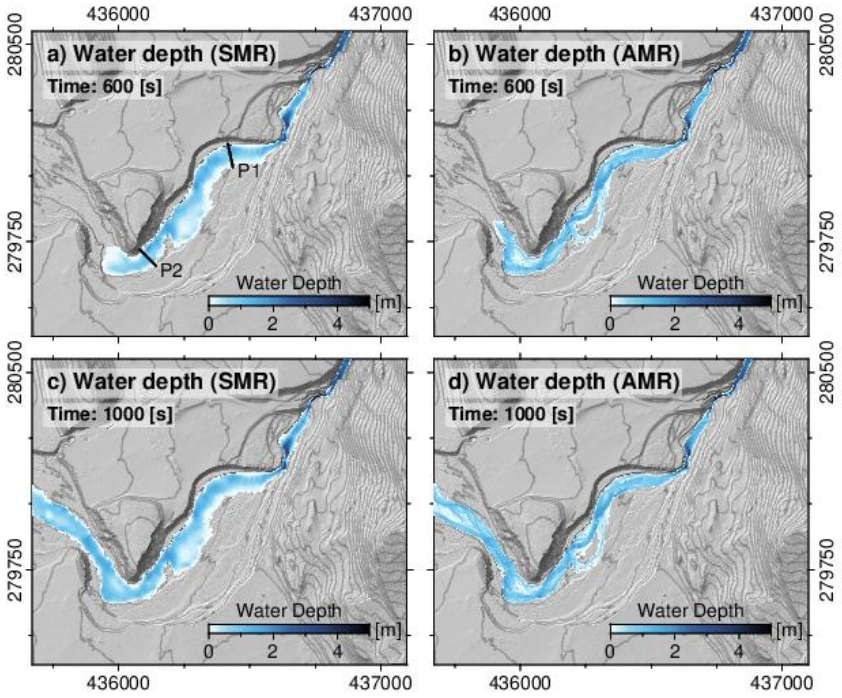

Figure 5: Water depth [m] after 600 [s] (above) and 1000 [s] (below) for simulations based on non-adaptive SMR (left) and AMR (right) quadtree grids. To provide better orientation, the position of the profiles (black lines) are displayed in a).

In addition, effects on the flow velocity can be observed due to the use of adaptivity. Figure 6 displays the resulting flow velocities along the two profiles (position visualized in Figure 5a). In simulations based on AMR, significantly larger fluctuations in velocity can be observed compared to SMR. It is apparent that the flow velocities along profile one reach significantly higher values when adaptivity is applied. Furthermore, the parts along the

profiles in which velocities are measured differ considerably between simulations based on SMR and AMR.

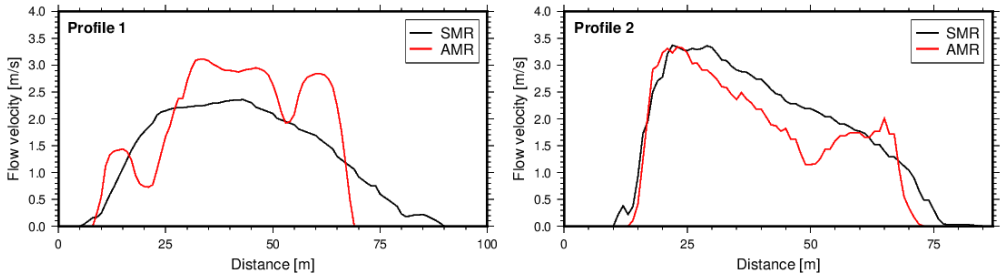

Figure 6: Flow velocity [m/s] after 1000 s along profile 1 (left) and 2 (right) for simulations based on SMR (black line) and AMR (red line).

Table 2: Inundated area [m²] resulting from simulations based on non-uniform SMR and AMR at different time steps [s].

Time [s]	Mesh refinement	Area [m²]
600	Static	87557.6
	Adaptive	72183.9
1000	Static	120312.9
	Adaptive	96313.7

4 Discussion

In line with the validation results presented by Stéphane Popinet (2012), a linear growth of the total amount of water in every time step results due to the constant discharge (Figure 2). Both hydraulic models are thus considered as valid. When comparing the simulated river course (Figure 5) and the non-uniform quadtree meshes (Figure 3), it is obvious that the SMR model fails to resolve the flood appropriately (i.e. with the maximum refinement level). This phenomenon is consistent with the results of Gong et al. (2020), who compared the accuracy of AMR models with a coarse SMR counterpart, among others. In contrast to a fine uniform grid in which the entire simulation domain is highly resolved, a non-uniform mesh based on two refinement criteria is used in this study. Consequently, the relevant flooded areas are not simulated with the highest resolution but mostly on a very coarse mesh. The predicted inundated area at the end of the simulation is therefore approx. 25 % larger in the SMR model. In contrast, the AMR model adapts the areas with the highest resolution to the evolving inundation as indicated by Qiuhua Liang et al. (2008).

In contrast to several studies (An et al., 2015; Gong et al., 2020; Qiuhua Liang et al., 2008; J. P. Wang & Liang, 2011), the results of this study have shown an increase in CPU time when AMR is applied (Figure 4). The reason for this is that those studies used the results of

a fine uniform non-adaptive quadtree grid for comparison. In this study, however, simulations based on non-uniform SMR are compared with an AMR model, whereby the results differ. According to recent studies (e.g., Huang et al., 2015; Qiuhua Liang et al., 2008), the required CPU time depends on the number of cells during the flood simulation. This observation is also reflected in the results of this study, as the AMR model requires about 54 % more CPU time as well as 35 % more cells than the SMR counterpart (Figure 4). Overall, adaptivity has a negative impact on computational costs when comparing the outcomes with a non-uniform SMR model. However, in accordance with J. P. Wang and Liang (2011), the increase in the number of cells visualized in Figure 4 indicates that the inundation is progressing (i.e. evolving flood). But the increase in the number of cells slows down after about 800 s since a constant discharge is fed into the simulation domain and a steady-state is reached at a certain time step (i.e. no further areas are flooded).

In accordance with the results presented by J. P. Wang and Liang (2011), who compared an AMR and a coarse uniform SMR model, the hydraulic parameters in this study do not show identical predictions of hydraulic parameters based on SMR and AMR at the data loggers (Figure 6). It is thus evident that the hydraulic model based on AMR, which consists of 35 % more cells than its non-uniform SMR counterpart, is more accurate in terms of information density.

5 Conclusion and Outlook

The aim of this study was to analyse and quantify the impacts on the computational efficiency of single flood simulations by applying AMR compared to a non-uniform SMR counterpart. The proposed 2D flood simulation models based on quadtree grids are applied to the torrent Taugl River located in the Salzburger Land. The comparison of the simulation results revealed that the AMR model requires 35 % more cells and 54 % more CPU time. However, since the lower cell amount in the non-uniform SMR model mainly results from the comparatively coarser grid in the flooded sites, the accuracy (i.e. the information density) of the analysed hydraulic parameters is quite inferior to the AMR model. Nevertheless, the accuracy of the predicted hydraulic parameters must be evaluated in future studies using field measurements. Several studies (e.g., Qiuhua Liang et al., 2007; J. Wang et al., 2004; J. P. Wang & Liang, 2011) have already approved the increase in the computational efficiency by using AMR compared to uniform SMR models. This study demonstrated that AMR models are also an improvement for flood simulations compared to a non-uniform SMR counterpart due to the better accuracy. However, this conclusion should be validated in future studies by applying different refinement criteria for the non-uniform SMR model. Furthermore, the impact of two factors on the results should be further investigated: 1) the implementation of a spatially variable bottom friction and 2) a temporal variable discharge.

Acknowledgements

I would like to thank Assoz.-Prof. Dr. Jörg Robl from the Department of Geology at the University of Salzburg for providing access to the used server and for important information regarding the hydraulic models.

References

An, H., & Yu, S. (2012). Well-balanced shallow water flow simulation on quadtree cut cell grids. *Advances in Water Resources, 39*, 60-70. doi:https://doi.org/10.1016/j.advwatres.2012.01.003

An, H., Yu, S., Lee, G., & Kim, Y. (2015). Analysis of an open source quadtree grid shallow water flow solver for flood simulation. *Quaternary International, 384*, 118-128. doi:https://doi.org/10.1016/j.quaint.2015.01.032

Anees, M. T., Abdullah, K., Nawawi, M. N. M., Ab Rahman, N. N. N., Piah, A. R. M., Zakaria, N. A., . . . Mohd. Omar, A. K. (2016). Numerical modeling techniques for flood analysis. *Journal of African Earth Sciences, 124*, 478-486. doi:https://doi.org/10.1016/j.jafrearsci.2016.10.001

Baynes, E. R. C., Attal, M., Niedermann, S., Kirstein, L. A., Dugmore, A. J., & Naylor, M. (2015). Erosion during extreme flood events dominates Holocene canyon evolution in northeast Iceland. *Proceedings of the National Academy of Sciences, 112*(8), 2355-2360. doi:10.1073/pnas.1415443112

Berger, M. J., & Oliger, J. (1984). Adaptive mesh refinement for hyperbolic partial differential equations. *Journal of Computational Physics, 53*(3), 484-512.

Bertram, M. H.-., & Tricoche, X. (2003). Adaptive Smooth Scattered Data Approximation for Large-scale Terrain Visualization. *The Eurographics Association*.

Borthwick, A., Cruz Leon, S., & Józsa, J. (2001). The shallow flow equations solved on adaptive quadtree grids. *International Journal for Numerical Methods in Fluids, 37*(6), 691-719.

Coulthard, T. J., & Van De Wiel, M. J. (2013). Numerical Modeling in Fluvial Geomorphology. In J. F. Shroder (Ed.), *Treatise on Geomorphology* (pp. 694-710). San Diego: Academic Press.

Darby, S. E., & Van de Wiel, M. J. (2003). Models in fluvial geomorphology. In G. M. kondolf & H. Piegay (Eds.), *Tools in fluvial geomorphology* (pp. 501-537). he Atrium, Southern Gate, Chichester, West Sussex PO19 8SQ, England: John Wiley & Sons.

Gong, W., Shimizu, Y., & Iwasaki, T. (2020). A Case Study of Flood Modeling with Adaptive Mesh Refinement. *Proceedings of the 22nd LAHR- APD Congress*.

Grenfell, M. C. (2015). Modelling Geomorphic Systems: Fluvial. In S. J. Cook, L. e. Clarke, & J. M. Nield (Eds.), *Geomorphological Techniques (Online Edition)*. London: British Society for Geomorphology.

Guttmann, M. (1997). *Das Tauglgebiet in der südwestlichen Osterhorngruppe.* Retrieved from https://permalink.obvsg.at/AC02156490

Hergarten, S., & Robl, J. (2015). Modelling rapid mass movements using the shallow water equations in Cartesian coordinates. *Nat. Hazards Earth Syst. Sci., 15*, 671-685. doi:10.5194/nhess-15-671-2015

Hou, J., Li, B., Tong, Y., Ma, L., Ball, J., Luo, H., . . . Xia, J. (2019). Cause analysis for a new type of devastating flash flood. *Hydrology Research, 51*(1), 1-16. doi:10.2166/nh.2019.091

Hu, R., Fang, F., Salinas, P., & Pain, C. C. (2018). Unstructured mesh adaptivity for urban flooding modelling. *Journal of Hydrology, 560*, 354-363. doi:https://doi.org/10.1016/j.jhydrol.2018.02.078

Hu, R., Fang, F., Salinas, P., Pain, C. C., Sto.Domingo, N. D., & Mark, O. (2019). Numerical simulation of floods from multiple sources using an adaptive anisotropic unstructured mesh method. *Advances in Water Resources, 123*, 173-188. doi:https://doi.org/10.1016/j.advwatres.2018.11.011

Huang, W., Cao, Z., Pender, G., Liu, Q., & Carling, P. (2015). Coupled flood and sediment transport modelling with adaptive mesh refinement. *Science China Technological Sciences, 58*(8), 1425-1438.

Keen, T. R., Campbell, T. J., Dykes, J. D., & Martin, P. J. (2013). *Gerris Flow Solver: Implementation and Application*. Retrieved from

Kesserwani, G., & Liang, Q. (2012). Dynamically adaptive grid based discontinuous Galerkin shallow water model. *Advances in Water Resources, 37*, 23-39. doi:https://doi.org/10.1016/j.advwatres.2011.11.006

Kirstetter, G., Bourgin, F., Brigode, P., & Delestre, O. (2020). Real-time inundation mapping with a 2D hydraulic modelling tool based on adaptive grid refinement: The case of the October 2015 French Riviera Flood. In *Advances in Hydroinformatics* (pp. 335-346): Springer.

Liang, Q., Borthwick, A. G. L., & Stelling, G. (2004). Simulation of dam- and dyke-break hydrodynamics on dynamically adaptive quadtree grids. *International Journal for Numerical Methods in Fluids, 46*(2), 127-162. doi:https://doi.org/10.1002/fld.748

Liang, Q., Du, G., Hall, J. W., & Borthwick, A. G. (2008). Flood inundation modeling with an adaptive quadtree grid shallow water equation solver. *Journal of Hydraulic Engineering, 134*(11), 1603-1610.

Liang, Q., Zang, J., Borthwick, A. G. L., & Taylor, P. H. (2007). Shallow flow simulation on dynamically adaptive cut cell quadtree grids. *International Journal for Numerical Methods in Fluids, 53*(12), 1777-1799. doi:https://doi.org/10.1002/fld.1363

Popinet, S. (2003). Gerris: a tree-based adaptive solver for the incompressible Euler equations in complex geometries. *Journal of Computational Physics, 190*(2), 572-600. doi:https://doi.org/10.1016/S0021-9991(03)00298-5

Popinet, S. (2004). Free computational fluid dynamics. *ClusterWorld, 2*(6), 7.

Popinet, S. (2012). Adaptive modelling of long-distance wave propagation and fine-scale flooding during the Tohoku tsunami. *Nat. Hazards Earth Syst. Sci., 12*(4), 1213-1227. doi:10.5194/nhess-12-1213-2012

Popinet, S. (2012). Karamea flood tutorial. Retrieved from http://gfs.sourceforge.net/wiki/index.php/Karamea_flood_tutorial

Smart, G. M., Duncan, M. J., & Walsh, J. M. (2002). Relatively Rough Flow Resistance Equations. *Journal of hydraulic engineering (New York, N.Y.), 128*(ISSN: 0733-9429), 578. doi:10.1061/(ASCE)0733-9429(2002)128:6(568)

Wang, J., Borthwick, A., & Taylor, R. E. (2004). Finite-volume-type VOF method on dynamically adaptive quadtree grids. *International Journal for Numerical Methods in Fluids, 45*(5), 485-508.

Wang, J. P., & Liang, Q. (2011). Testing a new adaptive grid-based shallow flow model for different types of flood simulations. *Journal of Flood Risk Management, 4*(2), 96-103.